Jurnal Teknologi

Full Paper

THE MAGNETIC FLUX DENSITY OF VARIOUS GEOMETRIES OF ROGOWSKI COIL FOR OVERVOLTAGE MEASUREMENTS

Ayob Nazmy Nanyan*, Mohamad Nur Khairul Hafizi Rohani, Muzamir Isa, Afifah Shuhada Rosmi, Ahmad Zaidi Abdullah, Baharuddin Ismail, Haziah Abdul Hamid

High Voltage Transient & Insulation Health (HVTrans) Group, Centre of Excellence for Renewable Energy (CERE), School of Electrical System Engineering, Universiti Malaysia Perlis (UniMAP), Pauh Putra Main Campus

Article history
Received
16 May 2019
Received in revised form
12 November 2019
Accepted
19 November 2019
Published online
25 December 2019

*Corresponding author
ayobnazmy@studentmail.unimap.edu.my

Graphical abstract

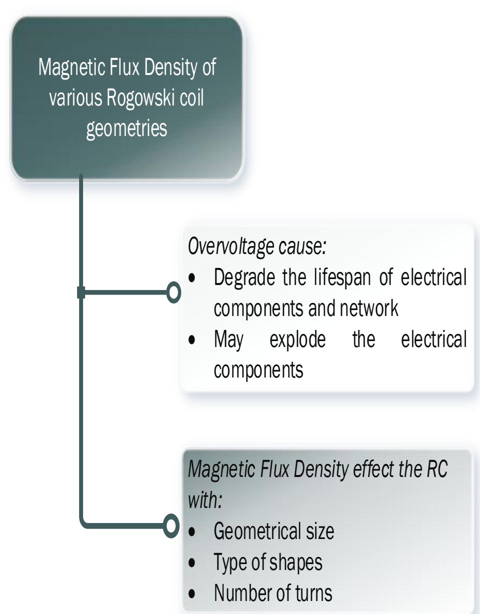

Abstract

Overvoltage phenomenon is the common problem that always occurs in the power system and can cause the electrical system network breakdown, and in some cases, it may explode. The frequent overvoltage also can affect and degrade the lifespan of the electrical power system components and network. Thus, the overvoltage sensor is needed to overcome this problem matter. The Rogowski coil (RC) is one of an inductive coil group, and it is suitable for measuring the alternating current (AC) and transient currents or overvoltage. This paper demonstrated the effect of RC magnetic flux density, B with difference cross-section, geometries sizing and the number of turns by using Finite Element Method (FEM). Commonly, there are three types of RC widely used; rectangular, circular and oval. Each of these cross-sections has different characteristics in term of performance. The results have shown that the rectangular cross-section is better than oval and circular cross-section based on the number of magnetic flux density.

Keywords: Overvoltage, Rogowski coil, Magnetic Flux Density, Finite Element Method (FEM)

Abstrak

Fenomena voltan lampau adalah masalah yang sering berlaku di dalam sistem kuasa dan boleh menyebabkan kegagalan rangkaian sistem elektrikal dan dalam sesetangah kes ia boleh menyebabkan letupan. Kekerapan voltan lampau boleh mengurangkan jangka hayat komponen sistem kuasa elektrik dan juga rangkaian. Maka, pengesan voltan lampau diperlukan untuk menyelesaikan masalah ini. Gegelung Rogowski (GR) adalah salah satu daripada kumpulan gegelung induktif dan ianya sesuai untuk mengukur arus ulang alik, arus fana atau voltan lampau. Artikel ini mendemonstrasi kesan ketumpatan fluks magnetic, B GR dengan perbezaan keratan rentas, saiz dan juga bilangan lilitan menggunakan analisis elemen terhad. Lazimnya, tiga jenis GR yang selalu digunakan ialah segi empat, bulatan dan bujur, dan setiapnya mempunyai sifat berbeza dari segi keupayaan. Hasil kajian menunjukkan bentuk segi empat adalah lebih baik dari bentuk oval dan bulatan berpandukan pada ketumpatan fluks magnet.

Kata kunci: Voltan lampau, Gegelung Rogowski, ketumpatan fluks magnet, analisis unsur terhingga

1.0 INTRODUCTION

Overvoltage is the voltage in a circuit that raised above its upper design limit, and this phenomenon can cause a voltage spike and lead to power surge, and the conditions may be hazardous. Overvoltages can be classified; *temporary overvoltages, slow-front overvoltages, fast-front overvoltages and very-fast-front overvoltages* and always occur to power systems such as faults, lightning strokes, switching operations, during energised and de-energised gas-insulated substations (GIS) or transformers and others [1]. The frequent overvoltages phenomenon will affect the electrical equipment such as give stress to the insulation, degrade the lifetime of the equipment and easily short circuit transformer winding [2]. The monitoring system for the overvoltage has many ways and has developed by other researchers, but improvement is still needed [3]–[5].

The Rogowski coil (RC) is an inductive coil group which was introduced by German physician Walter Rogowski in 1912 [6]. The RC has many advantages than high-frequency current transducer (HFCT); thus it is most suitable for high current, and partial discharge measurement sensor and the capability of the RC have proved by previous researchers [7]–[11]. The advantages of the RC is it can measure the transient current from a few amperes up to few hundred amperes, measure wide bandwidth, which is from a few Hz up to hundreds MHz [12]. The RC current sensors operate on the same principles as conventional iron-core HFCT, but the difference between these two is that RC windings are wounded above an air core, rather than over an iron core. Due to the absence of magnetic materials, RC has a linear characteristic [13]. The HFCT is a ferromagnetic core sensor [14], thus is has the saturation problems (if the core is saturated, the magnetic permeability will drop drastically, close to the air's permeability) [15]. The RC sensor output is proportional to the measured signal and classified as low-power standalone current sensors by the International Electrotechnical Commission (IEC). The relevant IEC standard is IEC 60044-8, which will soon be replaced by IEC 61869-10 [16].

The RC consists of wire wound on a non-magnetic core and the required current to be measured will flow through the core [17], and the structure of RC, as shown in Figure 1. For measuring the current, the RC placed around the conductor. A magnetic field generated as current flows around the conductor. This field converted into a signal according to Faraday's induction law, which is proportional to the current or equivalent to the rate of change of the current flowing in the conductor [17]. The parameters shown in Figure 1 described as follows: ' a ' is the inner radius (mm), ' b ' is the outer radius (mm), ' W ' is the thickness, and ' I ' is the current flows in the centre of RC perpendicularly.

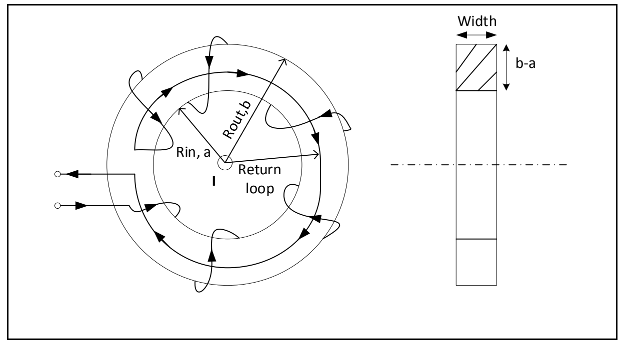

Figure 1 The structure of the Rogowski coil [18]

This paper aims to provide considerable knowledge when designing the RC as an overvoltage sensor application by referring to magnetic flux density before the sensor fabrication made. Subsequently, the RC cross-section assessment by mathematical approach proved that the circular cross-section is better than the rectangular cross-section inaccuracy of current measurement and reduce the angle error [19]. Indeed, in some cases, the rectangular cross-section is better than circular cross-section if the rectangular height per width is less than 0.4 and many researchers observed that the rectangular cross-section has higher sensitivity than other shapes cross-section of the RC [20], [16]. The main objective of this work is to analyse RC geometrical; oval, circular and rectangular by using Finite Element Method (FEM) method in term of magnetic flux density, B effect. Both of the rectangular and oval have observed with the changing effect of inner radius, outer radius, number of turns and area. To maintain the outer and inner radius which the same with oval and rectangular, the circle diameter of circular cross-section is adjusted, but the number of turns remains the same with both of the oval and rectangular.

Magnetic Field and Mutual Inductance

The mutual inductance, M changes in most of the actual coils, and it depends on electromagnetic parameters and geometrical. The magnetic flux Φ defined as the group of magnetic field lines emitted outward from the north pole of a magnet, and generally, a current-carrying wire produces the magnetic field around it and measured in Weber. The magnetic field intensity H and the magnetic flux density B at some defined point are in a reciprocal relation to the distance from the wire and the relationship between magnetic field intensity and magnetic flux density as expressed in Equation *1*. The μ_o is the absolute permeability of the medium and the value is $4\pi \times 10^{-7}$ H/m.

$$B = \mu_O . H = \frac{\mu_O . I}{2\pi . r} \qquad (1)$$

Initially, magnetic flux density B is the amount of magnetic flux per unit area of a section, perpendicular to the direction and this magnetic flux density also known as the magnetic induction, is a vector quality and the SI unit is in Weber/m^2 or Tesla (T). The magnetic flux density can be express as in Equation 2. A defines the area that magnetic density passes through.

$$\mathrm{B} = \frac{\Phi}{A} \qquad (2)$$

The magnetic flux density due to the entire current loop (which may be arbitrary), is at any point given by experimentally obtained by Biot-Savart law and as expressed by Equation 3. The unit vector a_r is directing from the source point or current element towards the field point (the point that we which determine B).

$$B = \frac{\mu_o}{4\pi} \oint_c \frac{IdI \times a_r}{r^2} \qquad (3)$$

Figure 2 presents a toroid that consists of a circular ring-shaped magnetic core around which wire is coiled. The magnetic field is entirely confined inside and the field points in the azimuthal direction.

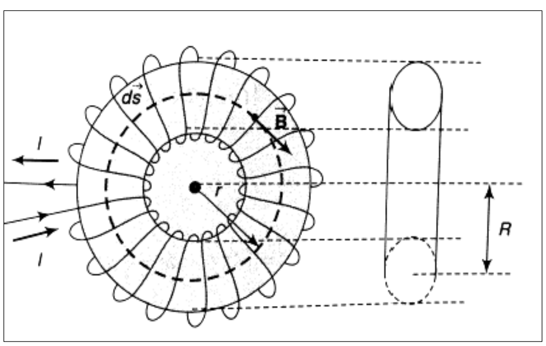

Figure 2 A toroid or Rogowski coil with N turns [21]

The coil sensitivity depends on the mutual inductance, M. The higher mutual inductance will produce higher sensitivity of RC. The characteristics of mutual inductance, self-inductance, self-resistance and self-capacitance of the RC coil are slightly different, and it is dependent on the coil geometry [22]. The mutual inductance slightly differs among the cross-section, where the geometrical sizing and number of turns N are the main factors. Typically, the mutual inductance calculated by using mathematical equation or formula [21]–[24]. Initially, better sensitivity can be achieved by adding a more considerable number of turns and with a broader cross-section of the coil [18]. However, the more significant number of turns may affect the performance of the RC, which will reduce the bandwidth of the RC. Moreover, increasing the number of turns also affect the length of the coil wire which the wire becomes longer and therefore, it will increase the capacitance value. As a result, it will produce a lower frequency resonant, and this case is not suitable for wide bandwidth application [24].

2.0 METHODOLOGY

In this paper, the RC modelling was developed using three dimensional (3D) FEM to concentrate on rectangular cross-section, circular cross-section and oval cross-section. It is well known that the magnetic flux depends on the geometric and number turns of these parameters. In this simulation, 5A current, which produces the magnetic field injected onto the cable. This idea, based on the theory where the wire that is carrying a current provides a magnetic field; thus, it is sufficient for analysis of the electromagnetic field due to the overvoltage phenomenon. Therefore, various geometrical size and number of turns simulated. Moreover, the effect of the wire diameter size (the wire that wounds around the RC) has investigated and analysed whether the magnetic flux is affected. The model consists of the geometric size of the RC, the cable as conductor and the wounded wire (turns) around the RC. Copper assigned as the cables in the simulation. Figure 3 shows the cross-section of rectangular, oval and circular RC which refer to the inner radius, Rin, outer radius, Rout, height and the area.

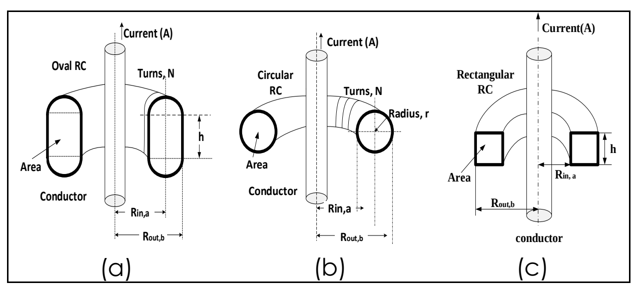

Figure 3 The cross-section of Rogowski coil; (a) Oval, (b) Circular (c) Rectangular

Table 1 shows the simulation parameters of the rectangular cross-section RC. The inner radius at 44 mm kept constant, while other parameters such as outer radius, height and width were varied. The surface area changed with the different height and width. Significantly, the sizing of the RC diameter was selected based on the underground three cores 240 mm^2 cross-linked polyethylene (XLPE) cable which has the overall diameter 76 mm [25] and this cable type also mainly used in power system [26]. Similarly, the circular cross-section of the RC, as shown in Table 2. In this case, the outer radius of circular and the number of turns has changed but the inner radius has remained. The same case shows in Table 3, where the modelling of the oval shapes for inner and outer radius follows the rectangular and circular size. This analysis was observed to study the effect between the density of magnetic flux, B and the number of turns which is to prove the theory that the magnetic flux density is directly proportional to the number of turns. Secondly, by increasing the geometrical size, the effect to the coil inductance and the length of the wounded wire and these factors were analysed and discussed.

Table 1 The Rectangular RC simulation parameters

Sensor	R_{in}, a (mm)	R_{out}, b (mm	Width (mm)	Height (mm)	Area (mm^2)
RT1	44	49	5	10	50
RT2	44	52	8	15	124
RT3	44	55	11	16	176
RT4	44	58	14	18	252
RT5	44	61	17	22	374
RT6	44	64	20	22	440
RT7	44	65	21	24	504
RT8	44	69	25	28	700
RT9	44	72	28	30	840
RT10	44	74	30	33	990

Table 2 The Circular RC simulation parameters

Sensor	R_{in}, an (mm)	R_{out}, b (mm)	Circle dia. (mm)	Area (mm)
CR1	44	49	5	19.6
CR2	44	52	8	50.2
CR3	44	55	11	94.4
CR4	44	58	14	153.8
CR5	44	61	17	226.8
CR6	44	64	20	314.0
CR7	44	65	21	346.2
CR8	44	69	25	490.6
CR9	44	72	28	615.5
CR10	44	74	30	706.5

Table 3 The Oval RC simulation parameters

Sensor	R_{in}, a (mm)	R_{out}, b (mm	Width (mm)	Height (mm)	Area (mm^2)
OV1A	44	49	5	10	44.6
OV2A	44	52	8	15	106.2
OV3A	44	55	11	16	149.9
OV4A	44	58	14	18	405.8
OV5A	44	61	17	22	318.2
OV6A	44	64	20	22	354.0
OV7A	44	67	21	24	430.2
OV8A	44	69	25	28	565.6
OV9A	44	72	28	30	671.5
OV10A	44	74	30	33	796.6

Figure 4 shows the modelling of the RC rectangular shapes in the simulation process and the similar procedure repeated with oval and circular. This model assumes that the RC sensor will detect a high-frequency signal which produced by a current signal that travels along the XLPE cable; the signal contents the magnetic field and the strength of the magnetic field depending on the current-carrying by the XLPE cable. Copper was assigned to the wire (wounded the RC) and also to the XLPE cable. Three shapes of the RC were model in this simulation work, and the observation of the magnetic flux on each shape was carried out and discussed in the next section. The geometry of each cross-section such as the inner radius remained constant (44 mm radius) for validation of magnetic flux density, and the other parameters were changed. The RC was model in 3D which consists of 240 mm^2 XLPE cable with N number of turns for the coil. This 3D FEM model is developed by computing the magnetic field through the Ampere's law which is uses multi-turn coil and meshing technique with triangle elements. Ampere's Law forms a frequency-domain for the magnetic and electric fields and the induced current that obtained in the FEM simulation, as shown in Equation *4* and *5*.

$$(j\omega\sigma - \omega^2\varepsilon_o\varepsilon_r)A + \nabla \text{x } (\mu_o^{-1}\mu_r B) - \sigma\omega \text{ x } B = J_e \quad (4)$$

$$B = \nabla \text{ x } A \quad (5)$$

Where ω is angular frequency, σ is electrical conductivity, ε_o and μ_o are the permittivity and permeability of free space respectively, A is the magnetic vector potential, ε_r is relative permittivity, μ_r is relative permeability, and J_e is the electric current density. The magnetic field strength, B is divergence-free in a constant magnetic field, and the magnetic vector potential A can be introduced to facilitate magnetic field calculation B.

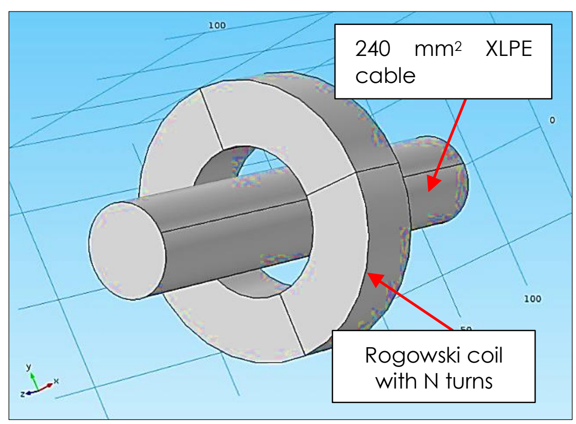

Figure 4 The 3D modelling of Rogowski coil in FEM software

Figure 5 shows the simulation flows of this work. There were 300 samples of RC designed and simulated using FEM. Each sensor has simulated in the range of 10 to 100 number of turns. Under this modelling, the magnetic flux density, B that presence surrounding XLPE cable and RC can also do analytically computed. From the simulation result, the graphs were plotted using the Minitab statics software.

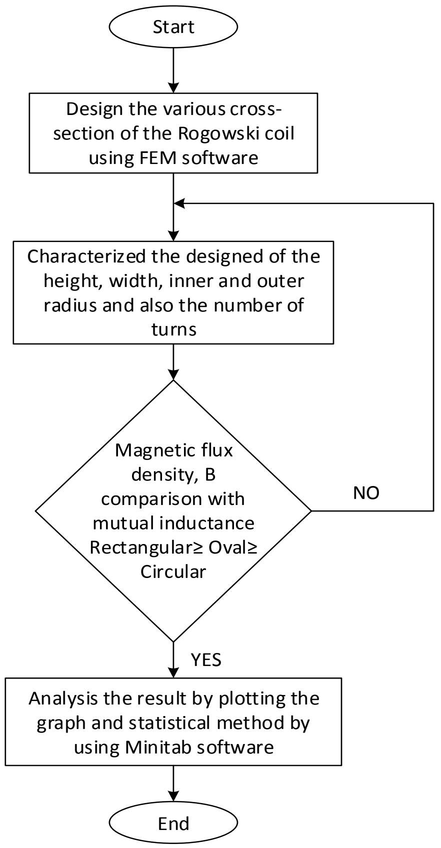

Figure 5 The flow process of simulation 3D RC

The significant of this simulation analysis is to prove that an electrical current that flows through a conductor creates magnetic field surround it. In this simulation, the magnetic flux density, B observed. Based on theoretical, winding the wire into a coil will increases the number of the magnetic flux lines, then increasing the field and therefore the inductance. Thus, the investigation was carried out to study the effect of magnetic flux density and coil inductance when the number of turns (winding) changed, and the geometrical shapes effect with the variable of the height, width, outer diameter and surface area by using FEM analysis. A suitable sensor indicated by the more magnetic flux density generates surrounding it, and the result has discussed in the next section.

3.0 RESULTS AND DISCUSSION

Previously, there were many researchers mentioned that the rectangular cross-section is better than circular and oval. The advantages of this analysis are that it makes it easier to determine the best shapes of the RC before fabricate. The result analysis focused on the geometrical effect, respectively. The finding of the study has discussed in this section. Many experts and scholars have analysed the performance and influence of the Rogowski coil, and researchers have demonstrated its feasibility for current measurement [27].

3.1 The Rectangular Cross-section Analysis

The sensitivity of the RC has a relation with the number of turns which improved significantly but will reduce the bandwidth of the RC. The performance in term of magnetic flux density analysis, as shown in Figure 6. The RT1 and RT2 have the highest magnetic flux between the RC, and the RT10 has the lowest magnetic flux density. In other words, the magnetic flux is not only dependent on the number of turns N, but other factors are influencing the magnetic flux density; it can say that a thin rectangular RC shape provides a high magnetic flux density and a broader cross-section provides a lower magnetic flux density. Some authors have found that Ampere's law makes a thin RC ideal to use as a transducer for alternating current measurement [28] and a similar finding have observed in this finding. By increasing the height and width of the RT10, the area increased to 990 mm^2 and the density of the magnetic flux drop rapidly. As the number of turns increased to 100 turns, the magnetic flux density of RT10 continued to decrease compared to others.

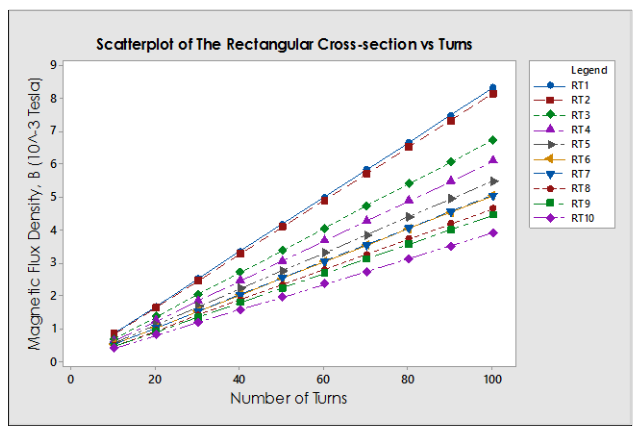

Figure 6 The Scatterplot of the Rectangular Cross-section RC

Meanwhile, the effects of the coil inductance are also studied when the surface area changed. The Meanwhile, the effects of the coil inductance are also studied when the surface area changed. The result analysis of coil inductance effects is, as shown in Figure 7.

From the obtained result, the area could also attribute to the coil inductance which the RT10 was producing the highest coil inductance (0.29 x 10^{-5} Henry and 29.2 x 10^{-5} Henry at 10 and 100 turns) compare to RT1 (0.04 x 10^{-5} Henry and 3.8 x 10^{-5} Henry at 10 and 100 turns). It is found that the increase in the surface area resulted in a significant increase in the inductance of the coil, as the wound wire becomes longer and at the same time raises the manufacturing costs. Theoretically, a coiled wire has a higher inductance than the same length straight wire because the lines of the magnetic field pass through multiple lines of the circuit that has multiple connections of flux. Thus, the result shows that the magnetic flux density increases with the number of turns, but the larger area of the RC does not produce high magnetic flux density.

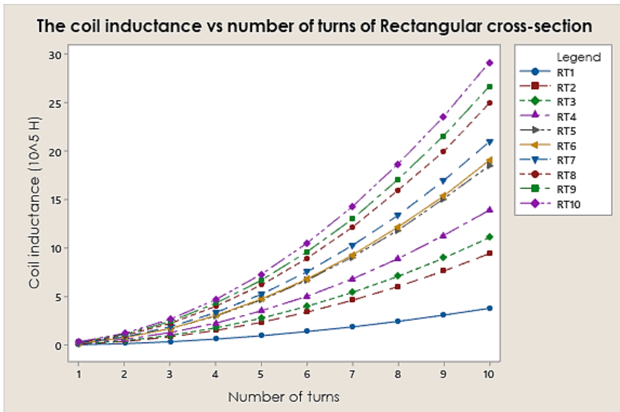

Figure 7 The coil inductance analysis over magnetic flux density of the rectangular cross-section

3.2 The Circular Cross-section Analysis

The geometric circular section has a different character with the rectangular section (the magnetic flux density was not depending on the area generally). Besides, all designed circular RC's magnetic flux density was lower than rectangular with the same geometric size. From the previous reason, the mutual inductance of the circular cross-section was not higher than rectangular [19]. The result analysis of a circular cross-section of magnetic flux density was plot as in Figure 8. As discussed earlier, better magnetic flux density generates by the higher value of N; magnetic flux density increased significantly. By expanding the N, all of the magnetic flux density of the circular RC increased. From the result obtained it shows that the CR3 produce the highest magnetic flux density among the others, which was recorded 6.07 x 10^{-3} T at 100 turns. In this case, the sensor analysis of the circular cross-section is challenging to determine because neither the magnetic flux density presence nor the geometric size and surface area reflected.

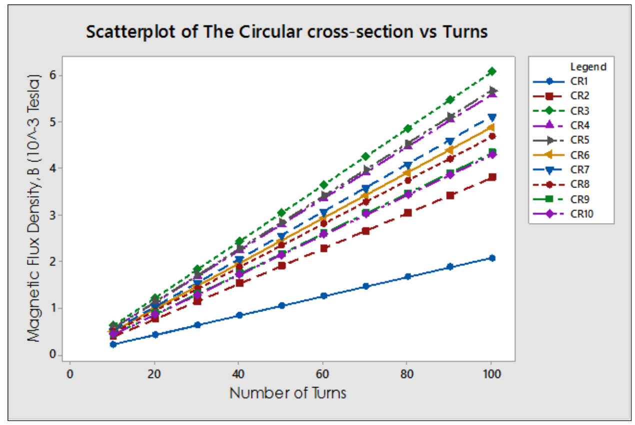

Figure 8 The magnetic flux density, B vs Number of turns of the circular cross-section Rogowski coil

The analysis of the geometric effect over the inductance coil, as shown in Figure 9 and the results obtained show that the coil inductance significantly increases when the surface area increases. By referring to CR3 case, the measured surface area was 94.4 mm^2 and produced a magnetic flux density of 6.07 x 10^{-3}T at 100 turns (the greatest among others) with 3.75 x 10^{-5} H as coil inductance. In another case, at 100 turns the CR1 (the lowest coil inductance) was only 0.30 x 10^{-5} H with the surface area 19.6 mm^2 while CR10 is the most significant surface area (706.5 mm^2) and 20.9 x 10^{-5} H coil inductance generated. It can see that better magnetic flux density not guaranteed in the circular cross-section by increasing or decreasing the surface area of the circular cross-section. When the surface area increased, the coil inductance automatically and expensively increases; the copper wire becomes more prolonged, and the cost of production significantly increases. As a conclusion, the magnetic flux density of the circular is seemed hard to determine by the surface area solely and therefore; an electromagnetic analysis is necessary when designing the circular RC cross-section.

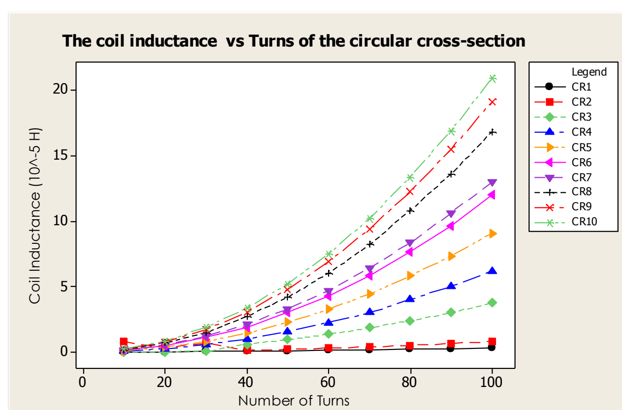

Figure 9 The coil inductance analysis over magnetic flux density of the circular cross-section

3.3 The Oval Cross-Section Analysis

The analysis was continued with the oval cross-section to compare the geometric effect of the RC extensively. Figure 10 shows the scatter plots of the oval cross-section with different number of turns and geometrical size. As can be seen, when increasing the number of turns results in significantly increased magnetic flux density for all sensors. The result showed that at 100 turns, the OV1A recorded the highest magnetic flux density (9.00 x 10^{-3} T) while the OV1A was the lowest (4.07 x 10^{-3}T), make it 75.44% difference. The analysis effect of the surface area found that the oval cross-section with thin and higher height; OV1A (44.6 mm^2) generated higher magnetic flux density than OV10A (796.6 mm^2) which was the most significant surface area.

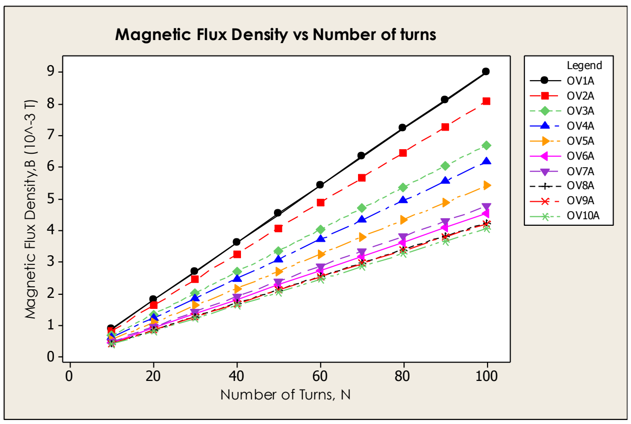

Figure 10 Scatter plot of the Oval cross-section coil

Meanwhile, when the surface area increased, it affected the coil inductance as well, and the simulation analysis is as shown in Figure 11. It can be seen that at 100 turns the OV1A coil inductance was 23.60 x 10^{-5}H while the OV10A was ascending to 100 x 10^{-5}H (the highest). This result indicates that by increasing the surface area, it did not contribute to improving the magnetic flux density, but only increases the coil inductance value increasing the wounded wire and production costs. Finally, a thin oval cross-section with a high number of turns and height produces a higher magnetic flux density than the large surface area.

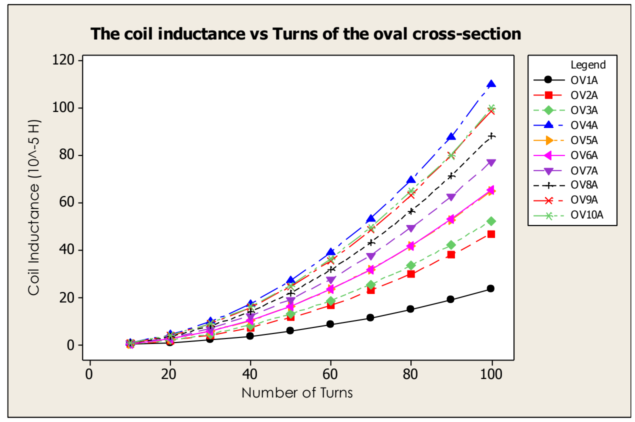

Figure 11 The coil inductance analysis over magnetic flux density of Oval cross-section

3.4 Summary of Geometrical Comparison

In summary, one of each group was selected and compared with the best cross-section (highest magnetic flux density); RT1, CR3, and OV1A. These cross-sections, however, have a different outer radius, width and consequently change the surface area and parameters as shown in Table 4.

Table 4 The parameters of OV1A, RT1 and CR3

Sensor	R_{in} (mm)	R_{out} (mm)	Surface area (mm^2)	Surface area changed %
RT1	44	49	50.0	-
CR3	44	55	94.4	88.8
OV1A	44	49	44.6	39.0

As can be seen in Table 4, the surface area of CR3 increased up to 88.8 % while OV1A was 39% over RT1, but the outer radius of RT1 and OV1A were equal. By using Minitab statistic tool, the analysis of variant (ANOVA) of the sensor design performance has applied, and the result, as shown in Figure 12. The cross-section 1 represented RT1, 2 represents CR3 and OV1A represented by 3. As shown in Figure 12 and Figure 13, the magnetic flux density of OV1A was higher than RT1, which was 7.35% better and 46.6% over CR3.

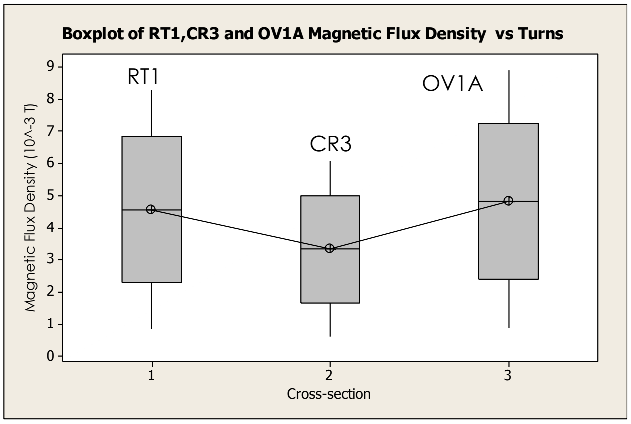

Figure 12 The analysis of variant (ANOVA) of the sensor design performance

However, by analysing the coil inductance in Figure 14, it was found that the coil inductance of RT1 was 3.80 x10^{-5}H lower than OV1A (100 x 10^{-5}H) at 100 turns. To achieve the high magnetic flux density, the surface area OV1A must be larger than RT1. Therefore, it needs to wrap with longer coil wire than RT1 and increasing the production cost. Consequently, in terms of price, RT1 is more reliable than OV1A. To sum up, the number of turns was proportional to the magnetic flux density and the inductance of the coil.

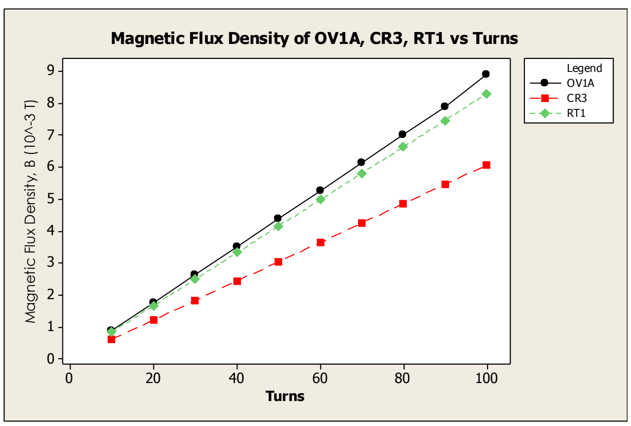

Figure 13 The comparison between the rectangular, oval and circular cross-section of magnetic flux density and turns

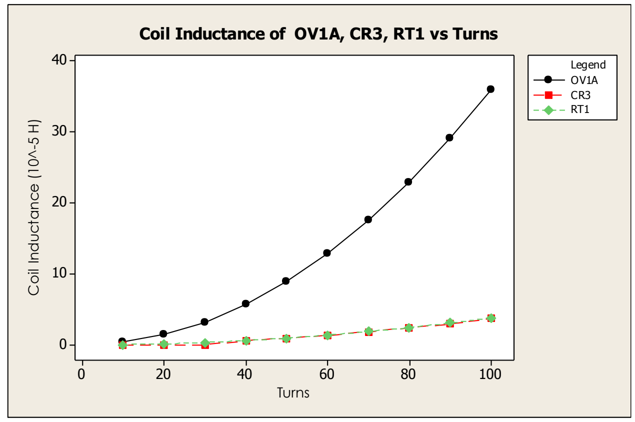

Figure 14 The comparison between the rectangular, oval and circular cross-section of coil inductance and turns

Table 5 The comparison between calculated mutual inductance and magnetic flux density, B (Rectangular cross-section)

Sensor	Number of turns, N	Mutual inductance, (Henry)	Magnetic Flux Density, (Tesla)
RT1	10	2.15 x 10^{-6}	0.83 x 10^{-3}
CR3	10	0.84 x 10^{-6}	0.61 x 10^{-3}
OV1A	10	2.99 x 10^{-6}	0.88 x 10-3

The comparison between calculated mutual inductance and magnetic flux density, B of RC cross-section simulation as shown in Table 5 which the comparison indicates that the magnetic flux density is in proportion with the mutual inductance; thus, this analysis is valid for the sensitivity analysis for Rogowski coil instead of conventional method by using mutual inductance calculation.

4.0 CONCLUSION

In this study, three different geometric cross-sections of the RC were presented and studied using the FEM analysis. By comparing the calculation method (mutual inductance), the 3D FEM analysis is more comfortable and more useful in determining the accuracy of the coil's magnetic flux density and inductance. The geometric effect and number of turns can be analyzed more easily using FEM. The simulation result shows that the rectangular cross-section is better than other simulated geometries in terms of magnetic flux density and cost. Some researcher suggested that the bandwidth depends on the number of turns where the bandwidth becomes lower if the number of turns increased and vice versa. Thus, the low bandwidth is not recommended for overvoltage measurement application. Therefore, the bandwidth performance must be considered as another factor for the design of the overvoltage sensor.

Acknowledgement

The author would like to thank the School of Electrical System Engineering, High Voltage Transient & Insulation Health Group (HV Trans) and Center of Excellence for Renewable Energy (CERE), Universiti Malaysia Perlis (UniMAP) for their support in improving this paper's quality.

References

[1] D. Sood and D. Sood. 2013. Reduction of Switching Over Voltages in H.V. Transmission Line. *Int. J. Sci. Eng. Res.* 5(6).

[2] Q. Yang, Y. Chen, W. Sima, and H. Zhao. 2016. Measurement and Analysis of Transient Overvoltage Distribution in Transformer Windings Based on the Reduced-scale Model. *Electr. Power Syst. Res.* 140: 70-77.

[3] Xiufang Jia, Shutao Zhao, Baoshu Li, and Wei Zhao. 2002. A New Method of Transient Overvoltage Monitoring for Substation. *Proceedings. International Conference on Power System Technology*. 2: 994-997.

[4] B. Filipović-Grčić. *et al.* 2017 Monitoring of Transient Overvoltages on the Power Transformers and Shunt Reactors–Field Experience in the Croatian Power Transmission System. *Procedia Eng.* 202: 29-42.

[5] M. Bi *et al.* 2016. Overvoltage Measurement based on the Electro-optic E-field Sensor. *2016 IEEE International Conference on High Voltage Engineering and Application (ICHVE)*. 1-4.

[6] M. H. Samimi, A. Mahari, M. A. Farahnakian, and H. Mohseni. 2015. The Rogowski Coil Principles and Applications: A Review. *IEEE Sens. J.* 15(2): 651-658.

[7] M. N. K. H. Rohani *et al.* 2016. Evaluation of Rogowski Coil Sensor Performance using EMTP-ATP Software. *2016 3rd International Conference on Electronic Design (ICED)*. 446-451.

[8] T. Kawabata, S. Yanagawa, H. Takahashi, and K. Yamamoto. 2015. Development of a Shunt Lightning Current Measuring System Using a Rogowski Coil. *Electr. Power Syst. Res*. 118: 110-113.

[9] Yi Liu, Fuchang Lin, Qin Zhang, and Heqing Zhong. 2011. Design and Construction of a Rogowski Coil for Measuring Wide Pulsed Current. *IEEE Sens. J.* 11(1): 123-130.

[10] T. B. Shulzenkho Eduard, Michael Rock, Josef Birkl. 2013. Specific By Measuring of Lightning Current with Large Rogowski Coil. *Int. Symp. Light. Prot. (XII SIPDA), Brazil*. 26-33.

[11] S. Tumanski. 2007. Induction Coil Sensors—A Review. *Meas. Sci. Technol*. 18(3): R31-R46.

[12] I. A. Metwally. 2010. Self-Integrating Rogowski Coil for High-Impulse Current Measurement. *IEEE Trans. Instrum. Meas.* 59(2): 353-360.

[13] C. L. G. Pavan Kumar *et al.* 2019. Development and Validation of Rogowski Coil with Commercial High-Frequency Current Transformer for Partial Discharge Detection. *Proceedings of 2018 International Conference on Electrical Engineering and Computer Science, ICECOS 2018*. 315-320.

[14] J. A. Ardila-Rey *et al.* 2018. A Comparison of Inductive Sensors in the Characterisation of Partial Discharges and Electrical Noise using the Chromatic Technique. *Sensors (Switzerland)*. 18(4): Apr.

[15] G. Bao, X. Gao, R. Jiang, and K. Huang. 2019. A Novel Differential High-frequency Current Transformer Sensor for Series Arc Fault Detection. *Sensors*. 19(17): 3649.

[16] P. Milovac, R. Javora, and V. Skendzic. 2017. Sensor Technology in Medium-voltage Switchgear for the US Market Applications. *CIRED - Open Access Proc. J*. 1: 432-435.

[17] L. A. Kojovic. 2007. Comparative Performance Characteristics of Current Transformers and Rogowski Coils used for Protective Relaying Purposes. *2007 IEEE Power Engineering Society General Meeting*. 1-6.

[18] L. Ferkovic, D. Ilic, and R. Malaric. 2009. Mutual Inductance of a Precise Rogowski Coil in Dependence of the Position of Primary Conductor. *IEEE Trans. Instrum. Meas.* 58(1): 122-128.

[19] M. Rezaee and H. Heydari. 2008. Mutual Inductances Comparison in Rogowski Coil with Circular and Rectangular Cross-sections and Its Improvement. *2008 3rd IEEE Conference on Industrial Electronics and Applications*. 1507-1511.

[20] I. A. Metwally. 2010. Self-Integrating Rogowski Coil for High-Impulse Current Measurement. *IEEE Trans. Instrum. Meas.* 59(2): 353-360.

[21] L. D. SP Ghosh. 2012. Magnetostatics. *Electromagnetic Field Theory*. New Delhi: Tata McGraw-Hill Education Private Limited. 288-289.

[22] M. Shafiq, G. A. Hussain, L. Kütt, and M. Lehtonen. 2014. Effect of Geometrical Parameters on the High-frequency Performance of Rogowski Coil for Partial Discharge Measurements. *Meas. J.* 49: 126-137.

[23] X. Liu, H. Huang, and C. Jiao. 2019. Modeling and Analyzing the Mutual Inductance of Rogowski Coils of Arbitrary Skeleton. *Sensors*. 19(15): 3397.

[24] M. N. K. H. Rohani *et al.* 2016. Geometrical Shapes Impact on the Performance of ABS-Based Coreless Inductive Sensors for PD Measurement in HV Power Cables. *IEEE Sens. J.* 16(17): 6625-6632.

[25] Universal Cable (M) Berhad. 2011. XLPE Insulated Power Cables. Retrieved from http://www.ucable.com.my/images/products/UC XLPE Catalogue.pdf.

[26] C. C. Yii, M. N. K. H. Rohani, M. Isa, and S. I. S. Hassan. 2017. Multi-end PD Location Algorithm using Segmented Correlation and Trimmed Mean Data Filtering Techniques for MV Underground Cable. *IEEE Trans. Dielectr. Electr. Insul.* 24(1): 92-98.

[27] Yi Li, Yunchen Guo, Yi Long, Chenguo Yao, Yan Mi, and Junfeng Wu. 2012. Novel Lightning Current Sensor based on Printed Circuit Board Rogowski Coil. *2012 International Conference on High Voltage Engineering and Application*. 334-338.

[28] D. A. Ward and J. L. T. Exon. 1993. Using Rogowski Coils for Transient Current Measurements. *Eng. Sci. Educ. J.* 2(3): 105.